



# High-power low spatial coherence random fiber laser

RUI MA,<sup>1,2</sup> JIA QI LI,<sup>1</sup> JIA YU GUO,<sup>1</sup> HAN WU,<sup>1</sup> HUA HUI ZHANG,<sup>1</sup> BO HU,<sup>1</sup> YUN JIANG RAO,<sup>1,3</sup> AND WEI LI ZHANG<sup>1,4</sup>

<sup>1</sup>Fiber Optics Research Centre, School of Information and Communication Engineering, University of Electronic Science and Technology of China, Chengdu 611731, China

<sup>2</sup>Aston Institute of Photonic Technologies, Aston University, Birmingham B4 7ET, United Kingdom

<sup>3</sup>yjrao@uestc.edu.cn

<sup>4</sup>wl\_zhang@uestc.edu.cn

**Abstract:** A high-power multi-transverse modes random fiber laser (RFL) is investigated by combining a master oscillator power-amplifier (MOPA) configuration with a segment of extra-large mode area step-index multimode fiber (MMF). Spatial coherence of the high-power multi-transverse modes RFL has been analyzed, which shows that speckle contrast is reduced dramatically with the output power increasing. In this way, considerably low speckle contrast of  $\sim 0.01$  is achieved under high laser power of  $\sim 56$  W, which are the records for multi-transverse modes RFLs in both spatial coherence and output power. This work paves a way to develop high-power RFLs with very low spatial coherence for wide-range speckle-free imaging and free-space communication applications.

© 2019 Optical Society of America under the terms of the [OSA Open Access Publishing Agreement](#)

## 1. Introduction

Random fiber lasers (RFLs) based on random distributed Rayleigh scattering and stimulated Raman scattering (SRS) are favorable for their stable output in time domain, simplicity in structure and reliability in practical applications [1–3]. Among all the potential applications, RFL with short fiber length is preferable for achieving highly efficiency/power output, while the optical-to-optical efficiency could approach the quantum limit [4,5]. Numerous researches on high-power RFLs have been put forward in recent years [6–9]. The output power of RFL based on short fiber length has been continuously promoted with the optimization of laser structures. More than 400 W RFL with good beam quality has been realized in a half-opened fiber structure, which is the record power of the state of art [10]. Moreover, the spectral bandwidth of the RFL has been demonstrated to be well maintained during high-power amplification in a master oscillator power-amplifier (MOPA) configuration that generates kilowatt-level RFL output [11].

Speckle-free imaging with low spatial coherence light source is also an attractive area in imaging applications that can be used to further improve the imaging quality and break through the resolution limit. Random lasers (RLs) generated from lasing process in disordered medium have been demonstrated to intrinsically possess low spatial coherence which is suitable for speckle-free imaging [12–15]. However, the applications of RLs are limited by its poor emission directionality and low output power. Therefore, fiber-optics based low coherence light sources are even more attractive in practical applications due to their high radiance in output power, excellent directionality in emission, flexibility in lasing wavelength and bandwidth [16,17]. Among the fiber-optics based light sources, multimode RFL has better imaging capability than conventional amplified spontaneous emission (ASE) source for its high spectral density under power-limited condition [18]. The evolutionary process of supercontinuum decoherence in extra-large mode area step-index multimode fiber (MMF) is also analyzed to provide high-quality broadband light source for speckle-free imaging [19]. However, the maximum output power of the recent reported low spatial coherence fiber laser

is relatively low, only about hundreds of milliwatts. Taking advantage of high brightness, high power laser with low spatial coherence could be used for speckle-free imaging, ghost imaging and free space communication [20,21], which can be realized by the combination of RFL and MMF.

In this letter, a high-power multi-transverse modes RFL with very low spatial coherence has been realized with maximum output power of  $\sim 56$  W and speckle contrast as low as 0.01. To realize this goal, a single-transverse mode RFL is firstly obtained with active gain of Ytterbium doped fiber (YDF), and its output is then amplified by a MOPA and injected into a segment of MMF to reduce the spatial coherence. Taking advantage of the high output power, more effective transverse modes (with high enough power to contribute to the final spatial coherence reduction) are excited in the MMF to reduce the spatial coherence. Meanwhile, the output of RFL keeps high spectral density even after amplification of the MOPA, which is of benefit to high-power speckle-free imaging. The all-fiber based amplification and decoherence configuration also provide a low-cost and reliable method to develop high-power low spatial coherence laser. This work not only advances RFL, but also greatly benefits those applications that need high-power light sources with very low spatial coherence.

## 2. Experimental setup and operation principle

Figure 1 gives the experimental setup of the high-power multi-transverse modes RFL. Single transverse mode RFL is generated through a MOPA configuration and further injected into MMF to reduce its spatial coherence. To realize random lasing, a conventional half-opened structure is used, which is composed of a high-reflectivity fiber Bragg grating (HR-FBG, central wavelength is 1064 nm, core/cladding diameters are 10/130  $\mu\text{m}$ ), 10 m length YDF (Nufern, core/cladding diameters are 10/130  $\mu\text{m}$ ) and 2 km length passive fiber (Corning, G.652). The gain is provided by active amplification in the YDF, while the optical feedback is provided by the point reflector of the HR-FBG and distributed Rayleigh scattering along the fiber. A laser diode (LD, 976 nm, core/cladding diameters of the output port fiber are 105/125  $\mu\text{m}$ ) is used as pump source and coupled into the structure through a  $(2 + 1) \times 1$  signal/pump combiner (core/cladding diameters of the signal port are 10/130  $\mu\text{m}$ ). A cladding power stripper (CPS, core/cladding diameters are 10/130  $\mu\text{m}$ ) is inserted between the YDF and the passive fiber to strip the unabsorbed LD pump light. A 1064 nm isolator (ISO, core/cladding diameters are 10/125  $\mu\text{m}$ ) is connected after the passive fiber to make sure all the feedback in the backward direction is from Rayleigh scattering.

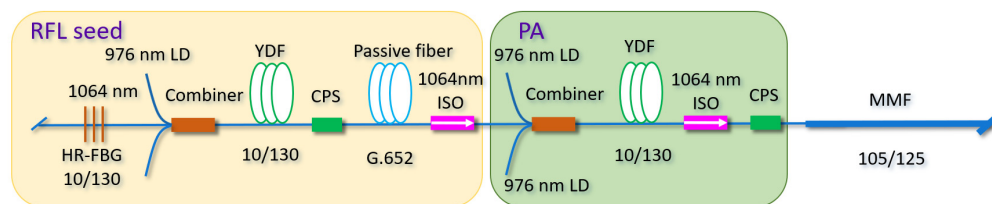


Fig. 1. Schematic diagram of experimental setup. HR-FBG, high-reflectivity fiber Bragg grating. LD, laser diode. YDF, Ytterbium-doped fiber. CPS, cladding power stripper. ISO, isolator. MMF, multimode fiber. RFL, random fiber laser. PA, power amplifier.

The generated random lasing works as seed light of the MOPA system. In the power amplifier (PA), two additional 976 nm LDs are combined as pump source through a  $(2 + 1) \times 1$  signal/pump combiner. The 10 m length gain fiber is the same YDF as that in the RFL seed part. A high-power 1064 nm ISO (core/cladding diameters are 10/125  $\mu\text{m}$ ) is connected after the YDF to prevent backward feedback light from the following structures, while a high-power CPS (core/cladding diameters are 10/130  $\mu\text{m}$ ) is also used to strip the unabsorbed pump light and makes sure only the 1064 nm lasing is used for the following test. The high-power ISO plays an important role in this structure since any tiny feedback from the flowing

parts would be notably amplified in the backward direction and damage the gain fiber or the former parts.

The amplified random-lasing is then injected into a segment of extra-large mode area step-index MMF (YOFC, core/cladding diameters are 105/125  $\mu\text{m}$ , NA is 0.22, 30 m length) to further reduce the spatial coherence. It is worth to mention that the end of the MMF is angle cleaved to prevent feedback. In this way, high-power multi-transverse modes RFL is obtained at the end of the MMF. The spatial coherence of the generated multi-transverse modes RFL is further evaluated by a piece of ground glass diffuser and an infrared camera (Xenics, Bobcat-640-GigE, with sufficient resolution to detect speckle patterns for both high and low spatial coherence cases) which is introduced in [18] in detail.

### 3. Results and discussions

Firstly, characteristics of the random-lasing seed light are investigated. A 1064 nm 1:99 coupler is temporarily connected after the 1064 nm ISO of the RFL seed part to measure the optical spectrum through the 1% port. Figure 2(a) shows the optical spectra of the random-lasing seed light measured at different pump power. The spectrum becomes stable after the pump power is higher than the threshold and the bandwidth gradually broadens with the increase of pump power. The 3dB bandwidth is  $\sim 0.5$  nm under pump power of 5.728 W. Total output power of the seed light is measured by a power meter (Thorlabs, S314C), at the angled fiber end of the 1064 nm ISO, as shown in Fig. 2(b). The threshold of the random-lasing is 0.573 W, which is relatively lower benefitting from the Ytterbium based gain mechanism. The output power is 1.986 W under pump power of 5.728 W. This Ytterbium based amplification is preferable for its lower lasing threshold considering the 2 km length passive fiber [22].

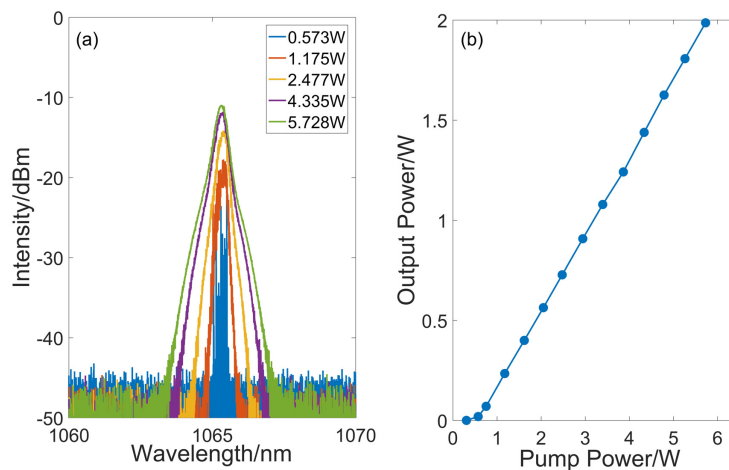


Fig. 2. (a) Optical spectra of the random-lasing seed light measured at different pump power. (b) Output power of random-lasing seed light versus pump power.

MOPA should be the most accessible method to realize high-power RFL, since high-power FBGs are not needed. Therefore, the random-lasing seed light is further amplified by the PA. Optical spectra and output power are analyzed at the output port of the CPS with the fiber end angle cleaved, as shown in Figs. 3(a) and 3(b) respectively. The bandwidth of the amplified random-lasing broadens slightly with the increasing of pump power, which is a notable characteristic comparing to conventional laser amplification process [11]. This can maintain the high spectral density feature of the RFL light source which is an advantage for speckle-free imaging with disordered medium [18]. The output power of the single-transverse mode random-lasing is measured through a high-power power meter. The maximum output

power reaches 56.2 W when the pump power of the amplifier is 90.2 W, which means the optical-to-optical efficiency is 62.3%, as is shown in Fig. 3(b). The original value of the optical-to-optical efficiency should be higher considering the insertion losses of the 1064 nm ISO and CPS. The output power after the amplification grows linearly with the increase of pump power. It shows that with further higher pump power, a much larger output power could be obtained.

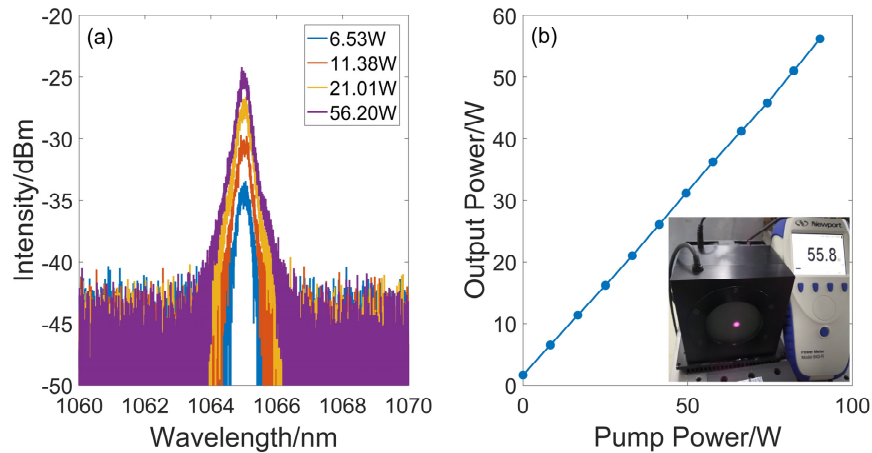


Fig. 3. (a) Optical spectra of the amplified RFL. (b) Output power of the incorporated pump power in the power amplifier. inset, photograph of the output power value after the amplified light is exported from the MMF.

Light radiating from single mode fiber has been demonstrated with high spatial coherence (high speckle contrast) [18]. To realize high-power RFL with multi-transverse modes, a spool of extra-large mode area step-index MMF is fusion spliced with the output port of the CPS, and the end of the MMF is also angle cleaved to prevent point feedback. The large modal dispersion of the step-index MMF provides one of the most efficient way for realization of low spatial coherence light. The maximum output power is 55.8 W for the maximum single-transverse mode RFL (56.2 W), as is shown in the inset of Fig. 3(b), photograph of the measured output power value from the end of MMF displayed on the power meter (Newport, Model 843-R).

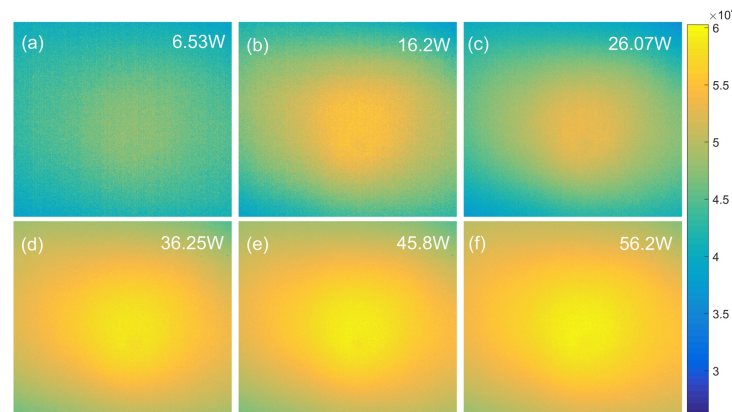


Fig. 4. Speckle patterns formed after light passing through a ground glass diffuser at different power.

The ability of speckle-free imaging can be connected by the value of speckle contrast  $C$  [12], which is inversely proportional to  $\sqrt{M}$  ( $M$  is the number of spatial modes) [23]. However, since the output power is too high for direct measurement, the lasing is firstly attenuated by a wedged plate beam splitter after exported from the MMF. Furthermore, absorptive neutral density filters are inserted before the light encounters with following imaging devices. The strength of this attenuation keeps unchanged during the following measurement process, where varied lasing power has been investigated.

The speckle patterns after the light passing through the ground glass diffuser under different light power are shown in Fig. 4. Speckles are only clearly visible in Fig. 4(a). With output power increasing, the intensity distribution of the speckle profile after the ground glass gets smoother and no evident speckles are visible in these higher power cases. Speckle contrast for different power is calculated from the measured speckle patterns [18]. It is worth to note that with the strong attenuations, the value of the calculated speckle contrast should be different from that of the original light source, since modes with lower power could be depleted and have no contribution to speckle reduction. On the other hand, due to the nonuniform power distribution of the excited transverse modes (lower order transverse modes have higher power than higher order modes), the modes with lower power that even passing through the depletion part could also contribute no role in the speckle reduction since the ground glass would also prevent the lower power light (due to the insertion loss of the ground glass). However, with the power further increasing, the number of effective modes (with high enough power to contribute to the final spatial coherence reduction) that pass the attenuation part also increases. In this way, the speckle contrast reduces greatly with more and more excited spatial modes contributing to the illumination, as shown in Fig. 5. Therefore, the measured value in Fig. 5 approaches the original value of the unattenuated light when the power is high enough. Speckle contrast of  $\sim 0.01$  has been obtained with  $\sim 56$  W output power, which also reflects high-power light in MMF can excite much more effective spatial modes than those in lower power regimes [18,19]. Therefore, increasing of the laser power could considerably improve the efficiency of decoherence process, since it could effectively reduce the spatial coherence for specified length of MMF. Additionally, spectral broadening induced decoherence effect has been investigated in previous work [19]. However, with spectral maintained MOPA technics, the minor spectral broadening here contributes little to the dramatic speckle contrast reduction as shown in Fig. 5. Thus, the principle reason here should be the increase of output power and the excitation of more effective transverse modes.

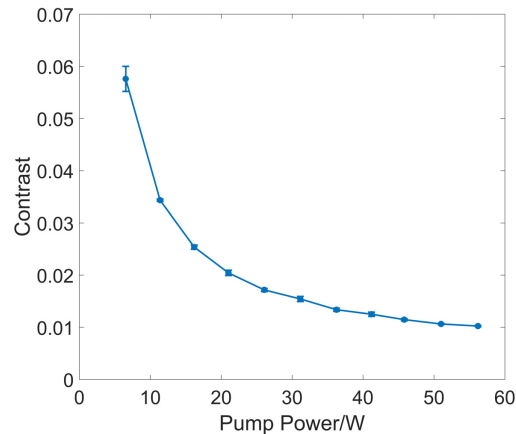


Fig. 5. Speckle contrast with variation range verse output power of RFL.

#### 4. Conclusions

High-power multi-transverse modes RFL with considerably low spatial coherence has been demonstrated with the combination of a MOPA configuration and a segment of extra-large mode area step-index MMF. The maximum output power is  $\sim 56$  W with speckle contrast as low as 0.01. This realization of high-power light source with low spatial coherence is preferable for its spectral bandwidth maintaining during the application process, which keeps the high spectral density of the random-lasing. Besides, the lower cost is also an advantage of the MOPA configuration, since high-power FBGs are not needed. Therefore, the proposed high-power multi-transverse modes RFL provides a powerful light source with considerably low spatial coherence, which would be well suitable for speckle-free imaging and free-space communication.

#### Funding

National Natural Science Foundation of China (NSFC) (61635005, 61575040, 61811530062); State 111 Project (B14039); China Scholarship Council (CSC) (201806070008).

#### Acknowledgments

The authors thank Jian Qiu Cao, Han Wei Zhang, Heng Chen, and Zhi He Huang for useful discussions and experimental guidance.

#### References

1. S. K. Turitsyn, S. A. Babin, A. E. El-Taher, P. Harper, D. V. Churkin, S. I. Kablukov, J. D. Ania-Castañón, V. Karalekas, and E. V. Podivilov, "Random distributed feedback fiber laser," *Nat. Photonics* **4**(4), 231–235 (2010).
2. S. K. Turitsyn, S. A. Babin, D. V. Churkin, I. D. Vatnik, M. Nikulin, and E. V. Podivilov, "Random distributed feedback fibre lasers," *Phys. Rep.* **542**(2), 133–193 (2014).
3. D. V. Churkin, S. Sugavanam, I. D. Vatnik, Z. Wang, E. V. Podivilov, S. A. Babin, Y. Rao, and S. K. Turitsyn, "Recent advances in fundamentals and applications of random fiber lasers," *Adv. Opt. Photonics* **7**(3), 516–569 (2015).
4. Z. Wang, H. Wu, M. Fan, L. Zhang, Y. Rao, W. Zhang, and X. Jia, "High power random fiber laser with short cavity length: theoretical and experimental investigations," *IEEE J. Sel. Top. Quantum Electron.* **21**(1), 0900506 (2015).
5. I. D. Vatnik, D. V. Churkin, E. V. Podivilov, and S. A. Babin, "High-efficiency generation in a short random fiber laser," *Laser Phys. Lett.* **11**(7), 075101 (2014).
6. S. A. Babin, E. I. Dontsova, and S. I. Kablukov, "Random fiber laser directly pumped by a high-power laser diode," *Opt. Lett.* **38**(17), 3301–3303 (2013).
7. H. Zhang, P. Zhou, H. Xiao, and X. Xu, "Efficient Raman fiber laser based on random Rayleigh distributed feedback with record high power," *Laser Phys. Lett.* **11**(7), 075104 (2014).

8. J. Xu, Z. Lou, J. Ye, J. Wu, J. Leng, H. Xiao, H. Zhang, and P. Zhou, "Incoherently pumped high-power linearly-polarized single-mode random fiber laser: experimental investigations and theoretical prospects," *Opt. Express* **25**(5), 5609–5617 (2017).
9. L. Zhang, J. Dong, and Y. Feng, "High-Power and High-Order Random Raman Fiber Lasers," *IEEE J. Sel. Top. Quantum Electron.* **24**(3), 1400106 (2018).
10. H. Zhang, L. Huang, P. Zhou, X. Wang, J. Xu, and X. Xu, "More than 400 W random fiber laser with excellent beam quality," *Opt. Lett.* **42**(17), 3347–3350 (2017).
11. X. Du, H. Zhang, P. Ma, H. Xiao, X. Wang, P. Zhou, and Z. Liu, "Kilowatt-level fiber amplifier with spectral-broadening-free property, seeded by a random fiber laser," *Opt. Lett.* **40**(22), 5311–5314 (2015).
12. B. Redding, M. A. Choma, and H. Cao, "Speckle-free laser imaging using random laser illumination," *Nat. Photonics* **6**(6), 355–359 (2012).
13. B. H. Hokr, M. S. Schmidt, J. N. Bixler, P. N. Dyer, G. D. Noojin, B. Redding, R. J. Thomas, B. A. Rockwell, H. Cao, V. V. Yakovlev, and M. O. Scully, "A narrow-band speckle-free light source via random Raman lasing," *J. Mod. Opt.* **63**(1), 46–49 (2016).
14. M. T. Carvalho, A. S. Lotay, F. M. Kenny, J. M. Girkin, and A. S. L. Gomes, "Random laser illumination: an ideal source for biomedical polarization imaging?" *Proc. SPIE* **9701**, 97010Q (2016).
15. Z. Hu, Q. Zhang, B. Miao, Q. Fu, G. Zou, Y. Chen, Y. Luo, D. Zhang, P. Wang, H. Ming, and Q. Zhang, "Coherent random fiber laser based on nanoparticles scattering in the extremely weakly scattering regime," *Phys. Rev. Lett.* **109**(25), 253901 (2012).
16. B. Redding, P. Ahmadi, V. Mogan, M. Seifert, M. A. Choma, and H. Cao, "Low-spatial-coherence high-radiance broadband fiber source for speckle free imaging," *Opt. Lett.* **40**(20), 4607–4610 (2015).
17. R. Ma, W. L. Zhang, S. S. Wang, X. Zeng, H. Wu, and Y. J. Rao, "Simultaneous generation of random lasing and supercontinuum in a completely-opened fiber structure," *Laser Phys. Lett.* **15**(8), 085111 (2018).
18. R. Ma, Y. J. Rao, W. L. Zhang, and B. Hu, "Multimode random fiber laser for speckle-free imaging," *IEEE J. Sel. Top. Quantum Electron.* **25**(1), 0900106 (2019).
19. R. Ma, W. L. Zhang, J. Y. Guo, and Y. J. Rao, "Decoherence of fiber supercontinuum light source for speckle-free imaging," *Opt. Express* **26**(20), 26758–26765 (2018).
20. J. C. Ricklin and F. M. Davidson, "Atmospheric turbulence effects on a partially coherent Gaussian beam: implications for free-space laser communication," *J. Opt. Soc. Am. A* **19**(9), 1794–1802 (2002).
21. S. Hartmann and W. Elsässer, "A novel semiconductor-based, fully incoherent amplified spontaneous emission light source for ghost imaging," *Sci. Rep.* **7**(1), 41866 (2017).
22. H. Wu, Z. Wang, Q. He, W. Sun, and Y. J. Rao, "Common-cavity ytterbium/Raman random distributed feedback fiber laser," *Laser Phys. Lett.* **14**(6), 065101 (2017).
23. J. W. Goodman, *Speckle Phenomena in Optics: Theory and Applications* (Roberts & Company, Englewood, 2007).